International Journal of Energy
ISSN: 2957-9473 | Vol. 2, No. 3, 2023

Experimental Study of the Behavior of Horizontally Buoyant Turbulent Jet Flames in Acoustic Waves

Ben Wang *, Qiang Wang

School of Automotive and Transportation Engineering, Hefei University of Technology, Hefei 230009, China

Abstract: Natural gas is most commonly transported by pipeline. However, leaks sometimes occur during transport, often leading to jet fires that cause substantial economic damage and property damage. It is therefore crucial to improve the efficiency of jet fire suppression. This paper focuses on the change of flame morphology of horizontal jet fires under different boundary conditions (acoustic pressure, frequency and jet exit velocity) and experimentally analyses the horizontal, vertical and trajectory length variation laws of the flame. Then a prediction model relating the horizontal length, vertical length and trajectory length of the horizontal jet flame under the action of acoustic waves is established.

Keywords: Jet Flame; Sound Waves; Flame Length.

1. Introduction

In a horizontal jet flame, the direction of buoyancy of the jet flame is perpendicular to the direction of the initial momentum of the fuel, which leads to a more complex coiled and turbulent flow field of the flame. This makes the flame behavior pattern of a horizontal jet flame significantly different from that of a vertical jet flame.

Tao et al. [1] and Liu et al. [2] proposed that the geometry of a turbulent diffusion jet flame changes as the tilt angle of the burner changes. Liu et al. [3-4] studied vertical upward and downward jet flames in the free condition and found significant differences in the shape characteristics of the two flames, and thus developed a model to predict the pattern of flame shape change. Liu et al. [5] found that when the flame is in the free condition and the initial tilt angle is oblique downward, the horizontal projection length of the flame decreases as the tilt angle increases, while the vertical flame length increases. Tao et al. [6] found that the parametric constant k of a diffusion jet flame changes with the initial tilt angle of the nozzle and developed a temperature profile model that takes into account the tilt angle of the nozzle. These studies have shown that the morphological characteristics of the jet flame change significantly as the nozzle angle is changed.

In the past decades, scholars have generally focused on flame instability and acoustic control during combustion, including thermoacoustic instability and oscillations in gas turbine combustion chambers and active control of flames [7-11]. Wang et al.[12] developed nonlinear response patterns of laminar diffusion flames to external perturbations at different acoustic frequencies. Li et al. [13] investigated the locking phenomenon of flame oscillations under acoustic waves and found that the oscillatory behaviour of flames is subject to acoustic Farhat et al. [14] found that the shape and behaviour of the flame is very sensitive to the phase of the standing wave generated by the loudspeaker and that the behaviour of the flame differs in different regions of the acoustic phase. The above studies suggest that the pulsation frequency and shape characteristics of the flame are influenced by the acoustic waves.

From a summary of the relevant studies above it is easy to see that horizontal jet flames and the lateral action of acoustic waves can introduce a great deal of complexity into the study of jet flame behaviour. There are a number of models that have analyzed the morphological changes of flames under vertical horizontal conditions, but the flame behaviour of horizontal jet flames under the action of acoustic waves has not been investigated. In this chapter, a series of experiments are conducted to investigate the flame morphological characteristics of horizontal buoyant turbulent jet flames under the action of transverse acoustic waves. A global model relating acoustic pressure to frequency is proposed for predicting the variation of horizontal jet flame trajectory length.

2. Experiment

The experimental setup for this paper is shown in Figure 1, with the nozzle facing the horizontal direction. The frequency is set at five points of 30Hz, 40Hz, 50Hz, 60Hz and 70Hz, and the sound pressure varies according to the shape of the flame until the flame is extinguished, with an interval sound pressure level of 2.5dB. The camera is set at the same level as the nozzle opening and facing the direction of the nozzle opening, and the speaker is also at the same level as the nozzle and perpendicular to the nozzle direction.

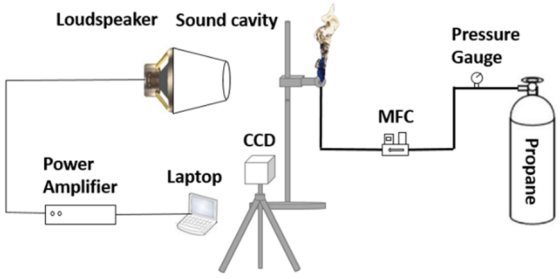


Fig 1. Diagram of the experimental set-up.

The experimental images were captured using a CCD camera (25 fps, 1920 x 1080 pixels). The raw flame images from the decompressed experimental video were first converted to grey scale and then converted to binary and average images using an image processing program. Finally, Tecplot 360 2013R1 software was used to plot a cloud map of the probability distribution of the flames. The flame probability profile is then obtained from the averaged flame binary image, with each length of the flame defined as shown

in Figure 2.

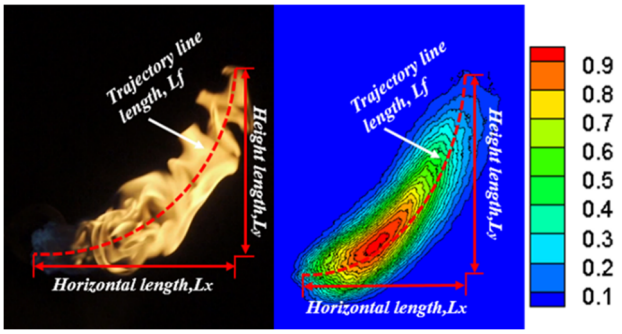


Fig 2. Definition of flame trajectory length (Lf) and flame height length (Ly) flame horizontal length (Lx)

3. Results and Discussion

Figure 3 shows the flame pattern at three different frequencies of 30Hz, 50Hz and 70Hz as a function of the transverse acoustic pressure when the fuel exit velocity is 16.99 metres per second. It is clear from the graphs that the flame at all frequencies gradually bends in the direction of acoustic propagation, and as the transverse acoustic pressure increases further, the bending of the flame increases and the flame trajectory length decreases in all cases. In addition, we can also find that the flames at the three frequencies show some variability with sound pressure. At a sound pressure level of 85 dB, the jet flame at 30 Hz already bends significantly, the flame at 50 Hz has not yet changed significantly, while the flame at 70 Hz still does not change significantly at a sound pressure level of 90 dB.

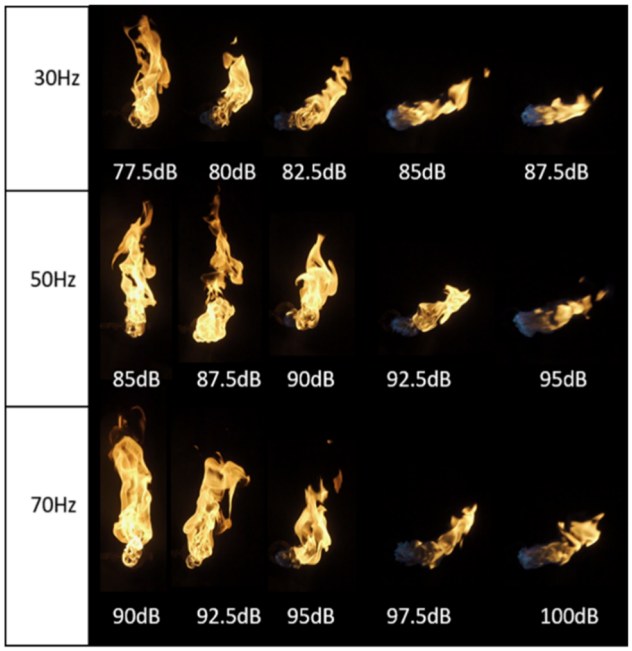


Fig 3. Variation of flame morphology with sound pressure at three frequencies for uj=16.99m/s

Figure 4 shows the trend of the jet flame trajectory length with the change of sound pressure and frequency of the transverse acoustic wave. As can be seen from the graph, the flame trajectory length decreases as the sound pressure increases, and the flame tends to decrease more slowly as the sound pressure increases to a certain level, at which point the flame gradually tends to go out. And at the same exit jet velocity and sound pressure, the lower the frequency the shorter the flame trajectory length. The end result of a shorter flame trajectory is extinguishment, so the above analysis shows that lower frequencies and higher sound pressures show better extinguishing effects.

The loudspeaker produces sound waves based on the vibration of the tympanic membrane, which produces airflow, the speed of which increases as the sound pressure increases. As the airflow increases, the mixing of fuel and air is intensified in the initial stages, resulting in faster fuel consumption. This leads to a further reduction in the length of the jet flame trajectory. In order to describe in more detail, the relationship between the morphological changes in the horizontal flame and the sound pressure frequency of the transverse acoustic wave, we have analyzed the experimental data in more detail below.

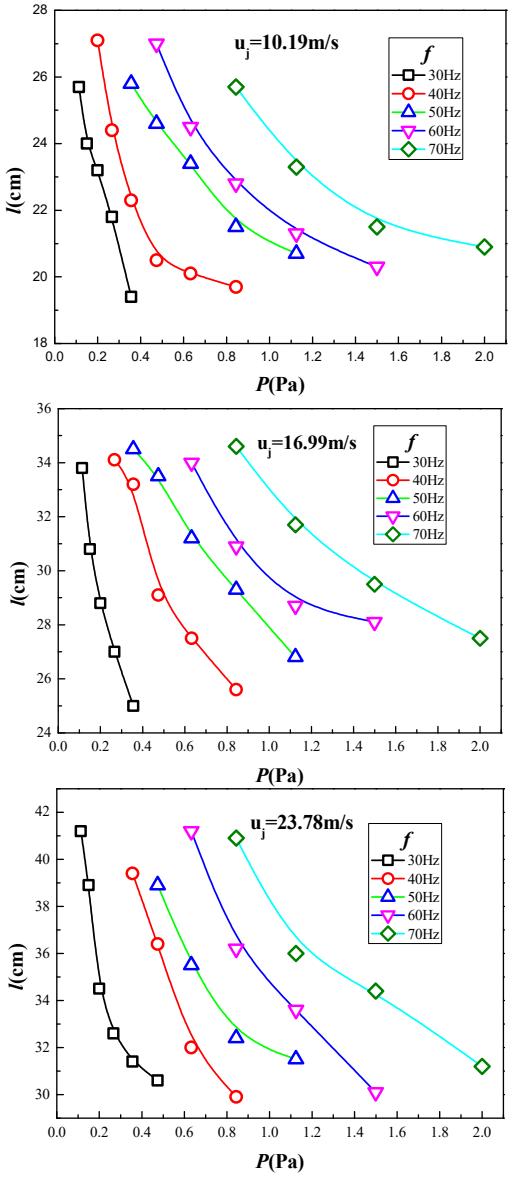


Fig 4. Variation of flame trajectory length with sound pressure at three fuel exit speed

3.1. Pattern of Change in Horizontal Flame Length

The flame length scale of a diffusion jet flame under free conditions should depend on the mutual coupling of fuel momentum and thermal buoyancy. Through extensive research of previous studies, it is not difficult to find that the flame length of a diffusion jet flame is determined by the

dimensionless parameter Froude number. In addition, Kalghatgi proposed a model for flame length variation considering the effect of wind and a dimensionless momentum ratio Rm, while zhang et al. developed a model to predict the horizontal length of a jet flame under the effect of ambient wind as follows:

$$\frac{L_x}{d} \propto f\left(R_M, Fr_\infty\right) \tag{1}$$

of which $Fr_\infty = \frac{u_\infty^2}{gd}$, $R_M = \left(\frac{\rho_j u_j^2}{\rho_\infty u_\infty^2}\right)^{1/2}$.

In this paper, we study the change in flame morphology under the action of acoustic waves, so we consider the conversion of the action of acoustic waves into the action of wind speed. xiong et al. introduced an equation for the conversion of acoustic pressure into wind speed when they studied an experiment using acoustic waves to extinguish a small burning wooden ball:

$$u_\infty = \sqrt{P/\rho} \tag{2}$$

In this paper, using the above equation, the sound pressure is quasi-commutated to the wind speed and then brought in for calculation. For a jet flame under the action of a transverse acoustic wave, the horizontal length of the flame should also be related to the frequency of the acoustic wave, so that there is:

$$\frac{L_x}{d} \propto f(R_M, Fr_\infty, f) \tag{3}$$

Based on the above equation the horizontal length of the jet flame at different frequencies under the action of transverse acoustic waves is shown in Figure 5. It is clear from the figure that the horizontal flame lengths at the same frequency show good normalization, while for different frequencies the horizontal flame lengths show some regularity. We fitted the difference in frequency into the original prediction model and obtained the correlation between the horizontal flame lengths of the jet flames at different frequencies as follows:

$$\frac{L_x}{d} = \left(-0.08f + 8.94\right)\left(R_M \cdot Fr_\infty\right)^{1/3} \tag{4}$$

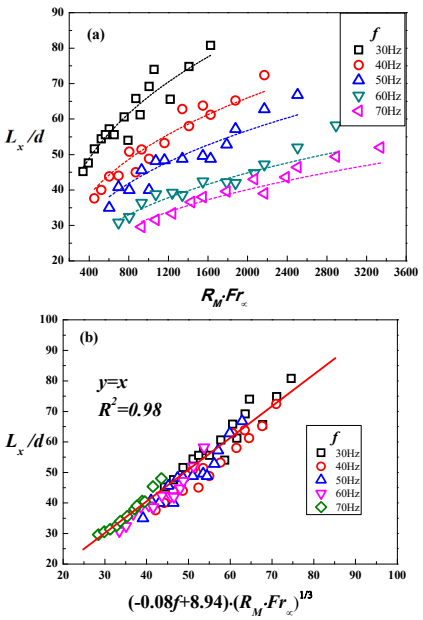


Fig 5. Relationship between the horizontal projection length of the flame and $R_M \cdot Fr_\infty$

3.2. The Pattern of Variation in Vertical Flame Length

Kalghatgi [15] found that the vertical flame height of buoyant jet fires under ambient winds was only related to the dimensionless momentum ratio:

$$\frac{L_y}{d} \propto f(R_M) \tag{5}$$

Again, we use the conversion of sound pressure to wind speed for this calculation, with frequency involved as another influencing factor, so that the vertical height of a horizontal jet flame under the action of transverse sound waves has:

$$\frac{L_y}{d} \propto f(R_M, f) \tag{6}$$

Figure 6 shows the relationship between the vertical flame length and the dimensionless momentum ratio RM for different frequencies. It is not difficult to find that the vertical flame height varies with RM with good normalisation for the same frequency, and with good regularity for data at different frequencies. We fitted the difference in coefficients between the different frequencies into the original model to obtain the following predictive model for the vertical flame length at different frequencies:

$$\frac{L_y}{d} = \left(0.31f + 3.04\right)R_M \tag{7}$$

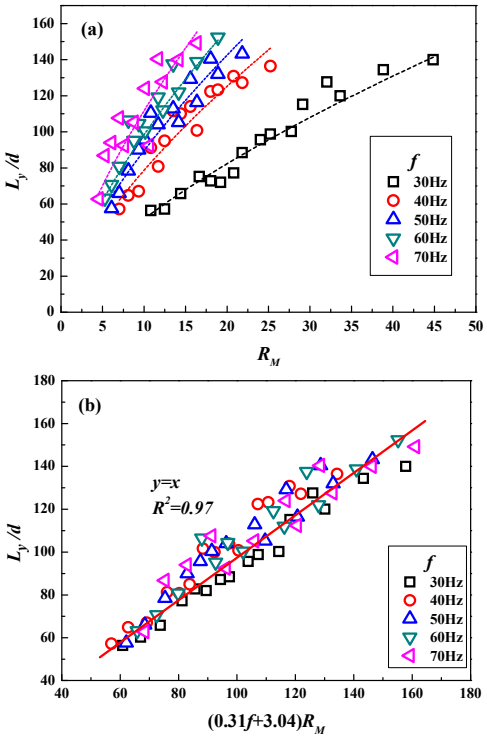


Fig 6. Relationship between vertical length of flame and RM

3.3. Pattern of Flame Trajectory Length Variation

A method for predicting flame trajectory length in windy conditions was found by Zhang et al. They obtained a predictive model for quantifying flame trajectory length by approximating the flame as a circular arc:

$$l_f = \sqrt{H_f^{\,2} + d_f^{\,2}}\,\frac{\frac{\pi}{2} - \operatorname{arccot}\frac{H_f}{d_f} - \operatorname{arccot}\frac{V_0}{V_s}}{\sin\left(\frac{\pi}{2} - \operatorname{arccot}\frac{H_f}{d_f} - \operatorname{arccot}\frac{V_0}{V_s}\right)} \tag{8}$$

Where l_f is the flame trajectory length, H_f is the vertical height of the flame, d_f is the horizontal projection line length of the flame, V_0 is the lateral wind speed and V_s is the fuel exit jet speed.

The model is a good predictor of flame trajectory length in windy conditions, and we apply the ideas of the model to consider the calculation of flame trajectory length in transverse acoustic conditions by combining the analysis with Figure 7.

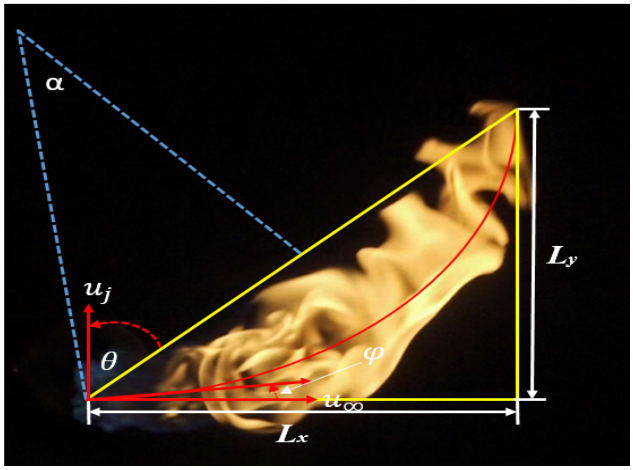


Fig 7. Typical flame trajectory diagram based on circular arc approximation assumptions

The position of the centre of the circle is determined by the intersection of two blue dashed lines (the vertical line in the direction of initial velocity at the source of the position line and the vertical centre line of the chord length). α is half the angle of the centre of the circle, u_f is the magnitude of the buoyancy of the jet flame, and u_∞ is the wind speed converted from sound pressure. From the diagram we can calculate that:

$$\theta = \operatorname{arccot}\frac{L_y}{L_x} \tag{9}$$

$$\varphi = \operatorname{arccot}\frac{u_\infty}{u_f} \tag{10}$$

This allows the following to be calculated for the hypothetical arc of the centre of the circle 2α and the radius R:

$$2\alpha = 2\left(\frac{\pi}{2} - \theta - \varphi\right) \tag{11}$$

$$R = \frac{\sqrt{L_x^{\,2} + L_y^{\,2}}}{2\sin\alpha} \tag{12}$$

The length of the trajectory line of the flame can then be obtained as follows:

$$L_f = \frac{2\alpha}{2\pi} * 2\pi R \tag{13}$$

Combining the above equations yields:

$$L_f = \sqrt{L_x^{\,2} + L_y^{\,2}}\,\frac{\frac{\pi}{2} - \operatorname{arccot}\frac{L_y}{L_x} - \operatorname{arccot}\frac{u_\infty}{u_f}}{\sin\left(\frac{\pi}{2} - \operatorname{arccot}\frac{L_y}{L_x} - \operatorname{arccot}\frac{u_\infty}{u_f}\right)} \tag{14}$$

By referring to the model fitted in the previous section concerning the vertical height of the flame and the horizontal length of the flame, we were able to calculate a prediction model for the length of the horizontal diffuse jet flame trajectory under the action of transverse acoustic waves, the results of which are shown in Figure 8. As can be seen from the figure, all the length data from this experiment fit this model well, and then this model is a good predictor of the change in the length of the horizontal jet flame trajectory under the action of transverse acoustic waves.

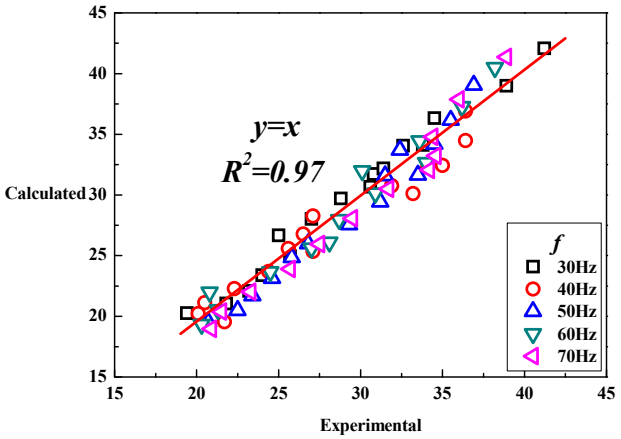


Fig 8. Comparison of experimental results with values calculated by Eq.

4. Conclusion

This chapter focuses on the experimental study of the variation of flame morphology of horizontal jet flames under the action of transverse acoustic waves. Quantitative models are derived for the variation of the horizontal projection length of the flame, the vertical height and the flame trajectory length. The main findings are as follows:

1. The evolution of the horizontal jet flame morphology under the action of transverse acoustic waves is studied. It is found that the flame trajectory length changes significantly with the change of sound pressure and frequency under the action of transverse acoustic waves, decreasing with the increase of sound pressure and showing a steep trend followed by a slow trend, while on the contrary, the flame trajectory length shows a decreasing trend with the increase of frequency. This leads us to conclude that for horizontal jet flames, lower frequencies and higher sound pressures are more effective.

2. The horizontal projection length and vertical height of horizontal jet flames under the action of transverse acoustic waves are investigated and two models are proposed to predict the horizontal and vertical length of horizontal jet flames under the action of transverse acoustic waves, with the help of previous research results for windy conditions.

3. Using the assumption of circular arc approximation, a model was developed to predict the length of the horizontal jet flame trajectory line under the action of transverse acoustic waves, and the model was able to fit well with all the data obtained from this experiment.

Acknowledgments

This work was supported jointly by Fundamental Research Funds for the Central Universities of China (No. JZ2022HGP A0310).

References

[1] Tao C, Shen Y, Zong R. Experimental determination of flame length of buoyancy-controlled turbulent jet diffusion flames from inclined nozzles[J]. Applied Thermal Engineering, 2016, 93: 884–887.

[2] Liu J, Wang J, Chen M. Estimating the trajectory length of buoyant turbulent jet flames issuing from a downward sloping nozzle[J]. Process Safety and Environmental Protection, 2019, 132: 153–159.

[3] Liu S, Hu L. An experimental study on flame envelope morphologic characteristics of downward-orientated buoyant turbulent jet fires [J]. Proceedings of the Combustion Institute, 2019, 37(3): 3935–3942.

[4] Liu S, Delichatsios M A, Hu L. Flame profile parameters of horizontal turbulent jets: Experiments, similarity analysis and an integral model [J]. Combustion and Flame, 2019, 207: 1–9.

[5] Liu J, Zhang X, Xie Q. Flame geometrical characteristics of downward sloping buoyant turbulent jet fires [J]. Fuel, 2019, 257: 116112.

[6] Tao C, Qian Y, Tang F, et al. Experimental investigations on temperature profile and air entrainment of buoyancy-controlled jet flame from inclined nozzle bounded the wall [J]. Applied Thermal Engineering, 2017, 111: 510–515.

[7] Steinbacher T, Albayrak A, Ghani A, et al. Response of premixed flames to irrotational and vortical velocity fields generated by acoustic perturbations [J]. Proceedings of the Combustion Institute, 2019, 37(4): 5367–5375.

[8] Kim K T, Lee J G, Quay B D, et al. Response of partially premixed flames to acoustic velocity and equivalence ratio perturbations [J]. Combustion and Flame, 2010, 157(9): 1731–1744.

[9] O'Connor J, Acharya V, Lieuwen T. Transverse combustion instabilities: Acoustic, fluid mechanic, and flame processes [J]. Progress in Energy and Combustion Science, 2015, 49: 1–39.

[10] Chen L-W, Wang Q, Zhang Y. Flow characterisation of diffusion flame under non-resonant acoustic excitation [J]. Experimental Thermal and Fluid Science, 2013, 45: 227–233.

[11] Hou S-S, Chung D-H, Lin T-H. Experimental and numerical investigation of jet flow and flames with acoustic modulation [J]. International Journal of Heat and Mass Transfer, 2015, 83: 562–574.

[12] Wang Q, Huang H W, Tang H J, et al. Nonlinear response of buoyant diffusion flame under acoustic excitation [J]. Fuel, 2013, 103: 364–372.

[13] Li L, Qiu T, Song D. Parameter estimation based on fractional power spectrum under alpha-stable distribution noise environment in wideband bistatic MIMO radar system [J]. AEU - International Journal of Electronics and Communications, 2013, 67(11): 947–954.

[14] Farhat S A, Ng W B, Zhang Y. Chemiluminescent emission measurement of a diffusion flame jet in a loudspeaker induced standing wave [J]. Fuel, 2005, 84(14): 1760–1767.

[15] Kalghatgi G T. The visible shape and size of a turbulent hydrocarbon jet diffusion flame in a cross-wind [J]. Combustion and Flame, 1983, 52: 91–106.